

# Experiments and FEM models on semi-composite behavior of SRC structures

メタデータ	言語: eng 出版者: 公開日: 2017-12-22 キーワード (Ja): キーワード (En): 作成者: メールアドレス: 所属:
URL	<a href="http://hdl.handle.net/2297/00049518">http://hdl.handle.net/2297/00049518</a>

This work is licensed under a Creative Commons Attribution 3.0 International License.



# EXPERIMENTS AND FEM MODELS ON SEMI-COMPOSITE BEHAVIOR OF SRC STRUCTURES

TAKAYUKI MATSUTA<sup>1</sup>, MIKIO KITAJIMA<sup>1</sup>, KOJI MAEGAWA<sup>2</sup>

<sup>1</sup>Graduate School of Natural Science & Technology, Kanazawa University, Kanazawa, Japan

<sup>2</sup>Faculty of Environmental Design, Kanazawa University, Kanazawa, Japan

Analytical models were prepared and results from these models were compared with experimental results to confirm the adequate modeling of steel-reinforced concrete members used in rockfall-protection galleries or rock-sheds. Static loading tests of steel-reinforced concrete members (a girder and a slab) were conducted on a simply supported beam. The analytical models have different contact conditions to verify which condition can express a semi-composite behavior and shear slide. Three types of contact conditions were applied: normal, tied, and tiebreak contact. Tiebreak contact can express the occurrence of gaps by defining shear bond strength. Consequently, analytical models that applied tiebreak contact showed comparatively good agreement with experimental results. Analytical models that applied the tiebreak contact condition showed a correlation of 97% (girder) and 101% (slab) with the experimental results for the maximum load-carrying capacity. Therefore, considering that slippage occurs between different materials, the model is good for expressing the behavior of complicated structures such as steel-reinforced concrete members that are used as a rock-shed.

*Keywords:* LS-DYNA, Static loading test, Contact condition, Rockfall-protection gallery, Rock-shed, Shear bond strength.

## 1 INTRODUCTION

Rock-sheds are the most reliable structures for protection from rockfall, and they require a high energy-absorption performance. They are made mainly from reinforced-concrete (RC) or prestressed-concrete (PC) structures. However, RC or PC members lose their strength rapidly after concrete failure and yielding of rebars and PC tendons, which is caused by the impact load of rockfalls. Steel-reinforced concrete (SRC) members that are composed of H-shaped steels and rebars can have a high toughness. Therefore, the high toughness of SRC structures is suitable for rock-sheds. Furthermore, the application of a SRC structure to rock-sheds can save on construction costs. SRC members have been used in some bridges, and studies have been conducted on these applications (Fukada, Kajikawa, and Tokuno 2008).

Test SRC members (a girder and a slab) were fabricated; these consisted of a SRC rock-shed. To confirm the specimen behavior, static loading tests were conducted on a simply supported beam. In this study, nonlinear finite-element analysis was conducted to understand the behavior in more detail. Some analyses of RC rock-sheds have been conducted (Bhatti and Kishi 2010). However, it is difficult to express the behavior of complex structures such as the SRC rock-shed, in particular because the contact conditions are intricate. Therefore, analytical models with different contact conditions were developed. These models were compared with experimental

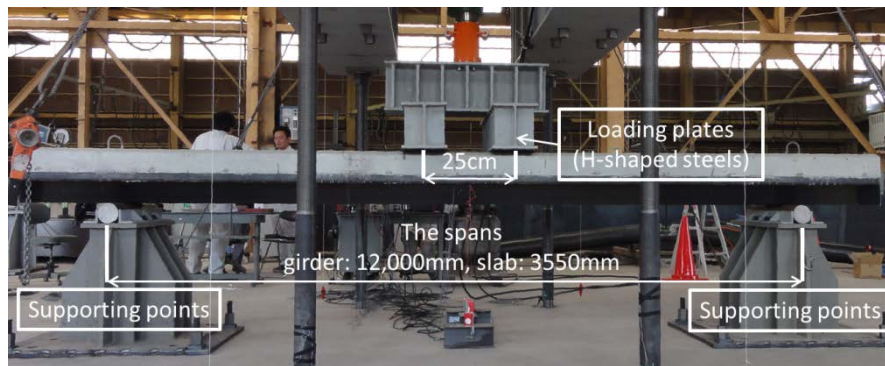
results to verify adequate contact conditions. Implicit analysis was carried out by using the non-linear analysis code, LS-DYNA.

The application of tiebreak contact to interfaces between steels and concrete materials showed good agreement with experimental results. Moreover, the tiebreak contact represents gaps between the interfaces.

## 2 OUTLINE OF STATIC LOADING TESTS

### 2.1 Experimental Equipment

Photograph 1 shows the experimental equipment that was used for the static loading tests. A test specimen was placed in the experimental equipment (loading capacity of 2500 kN and stroke of 30 cm). Two H-shaped steels (flange width of 200 mm) were placed on the specimen at 25-cm intervals, and they were used as loading plates. The static load was measured by using a loadcell. The displacement was measured by the stroke of a jack and two types of displacement gauges (wire and piston). The specimen strain was measured by strain gauges at outer steel plates, rebars, H-shaped steels, and concrete in the middle span.



Photograph 1. Experimental equipment for static loading tests.

### 2.2 Specimens

Figures 1 and 2 show cross-sectional views of the specimens. Outer steel plates were made, and their thicknesses were 6 mm (for the girder) and 4.5 mm (for the slab). Concrete was covered with the plates to protect pedestrians and vehicles from separate concrete blocks. H-shaped steel (H-692 × 300 × 13 × 20 (girder) and H-200 × 150 × 6 × 9 (slab)) and tensile rebars (12-D35 (girder) and 2-D16 (slab)) were placed inside the plates. Rock-sheds do not have to be complete composite structures like bridges because the design load does not work on the rock-sheds continually. Thus, headed studs (16 × 80 (girder) and 13 × 50 (slab)) were welded to the steel plates and H-shaped steels. Six or four studs were welded to the outer steel plates, and two or four studs were welded to the H-shaped steels at 1-m intervals at the testing girder; two-headed studs were welded to the outer steel plates and the H-shaped steel at 0.8–1-m intervals at the testing slab. The specimen lengths were 13 m (girder) and 4.9 m (slab), and the spans were 12 m (girder) and 3.55 m (slab). For the testing girder, casting concrete in an area under the H-shaped steels was difficult because the tensile rebars (D35 × 4800) were closely spaced in this area. Therefore, no-contraction mortar (compressive strength of 92.0 MPa) was cast up to 90 mm from the lower edge of the outer steel plates. Next, cast-in-place concrete (compressive strength of

52.5 MPa) was cast on the mortar. For the testing slab, cast-in-place concrete (compressive strength of 29.4 MPa) was cast on the precast concrete. Because casting of the cast-in-place concrete and the precast concrete yielded a time lag, cohesion of their interface was weak. Therefore, angle dowels (L50 × 50 × 6) were welded to the H-shaped steel, and dowel bars (D13 × 135) were placed near their interface at 1-m intervals to improve their cohesion. Distributing bars (25-D13 × 740) and compression rebars (4-D19 × 4840) were placed in the cast-in-place concrete at 200-mm intervals. Tensile rebars (2-D16 × 4800) were placed on the upper side of the lower flange of the H-shaped steel at 90-mm intervals in the precast concrete. The slab needs a high bending deformation capacity and the girder needs a high load-carrying capacity as well as the high bending deformation capacity.

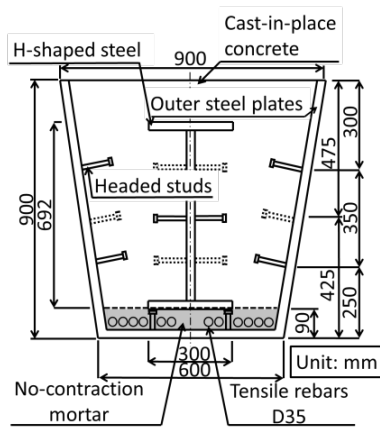


Figure 1. A cross-sectional view of the girder.

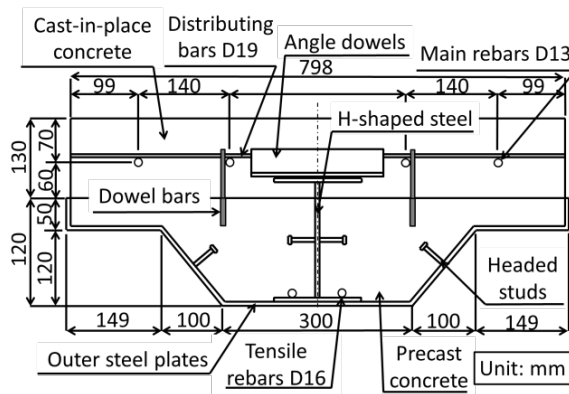


Figure 2. A cross-sectional view of the slab.

### 3 EXPERIMENTAL RESULTS

Photographs 2 and 3 show situations under which the static loading tests were conducted. The outer steel plates that caused buckling under compression occur in the middle span. The buckling resulted in a separation between the concrete and the outer steel plates. Furthermore, concrete at the upper edge was crushed near the loading plates. Connection steels (angle dowels and dowel bars) were introduced for the testing slab to inhibit slippage between the precast and cast-in-place concrete. However, with an increase in loading force, the cast-in-place concrete formed lateral gaps toward the left side of Picture 3. The maximum load-carrying capacities were 1791 kN (girder) and 526 kN (slab).



Photograph 2. A static loading test (girder).



Photograph 3. A static loading test (slab).

#### 4 OUTLINE OF ANALYTICAL MODELS

Figures 3 and 4 show the cross-sectional views of an analytical model of the specimens. The element sizes of the member axis were 44–50 mm (girder) and 25 mm (slab). The sums of the nodes and elements of the girder were 118,203 nodes and 87,744 elements. The sums of the nodes and elements of the slab were 88,916 nodes and 64,282 elements. The occurrence of gaps between the H-shaped steel and concrete materials influences the analytical model results. Therefore, three models were constructed to confirm the effect of a contact condition between the H-shaped steel and concrete materials with the only difference between the models being the tiebreak, tied, and normal contact conditions, which were denoted models S (shear), T (tied), and N (normal), respectively. Normal contact permits surface separation and does not permit penetration. Tied contact does not permit separation and surfaces maintain contact. Tiebreak contact is switchable from tied to normal contact. When interfacial shear stress is under shear bond strength that is inputted in advance, this contact is tied contact. However, after reaching the shear bond strength, this contact changes to normal contact. Therefore, tiebreak contact can express the occurrence of gaps. With regards other interfaces, the tiebreak contact is applied to two interfaces to consider the occurrence of gaps because of a difference in materials. The difference was between the precast concrete or no-contraction mortar and cast-in-place concrete, and the outer steel plates and concrete materials. The shear bond strength was 0.5 MPa at the interface between the steel and concrete materials (Committee on Hybrid Structures 2014) and 1.0 MPa at the interface between the concrete materials (Yasui 2010). In addition to the three models, model A (All) was developed. In this model, a tied contact was applied to all interfaces (outer steel plates, H-shaped steel, and concrete materials). Four models were compared with the experimental results. Besides the analytical model of the slab, a model was developed to confirm effect of connection steels (angle dowels and dowel bars); in this model, connection steels were removed from model S. The model was denoted model S-without and its output was compared with the experimental result.

A material model that can express softening was applied to the concrete materials (precast concrete, cast-in-place concrete, and no-contraction mortar). An isotropic elasto-plastic model was applied to the steel materials. An elastic and a rigid model were applied to the supporting points and the loading plates. Displacement controlling of the loading plate can be used to express static loading tests.

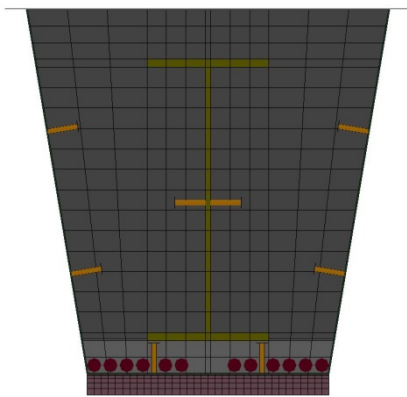


Figure 3. A cross-sectional view of an analytical model of the girder.

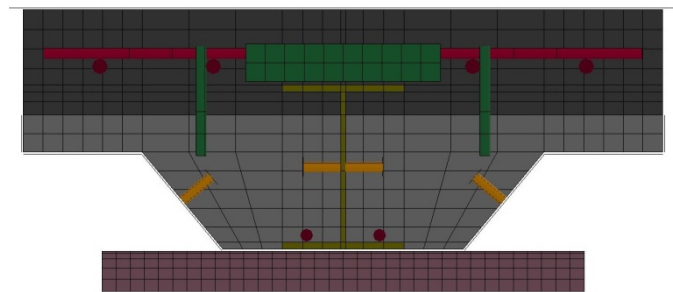


Figure 4. A cross-sectional view of an analytical model of the slab.

## 5 NUMERICAL RESULTS AND DISCUSSION

### 5.1 Testing Girder

Figure 5 shows the load–displacement relationship of the testing girder. The analytical results are somewhat unstable near the maximum load. These results are considered to occur because of slippage of the interface between the outer steel plates and supporting points. The load is calculated by the summation of nodal forces at the lower side of supporting points. Therefore, the slippage affects the load–displacement relationship.

Model S shows good agreement with the experimental result in terms of the maximum load-carrying capacity and softening behavior. In the elastic region, the stiffness of the numerical results is higher than that of the experimental result to about 750 kN. However, differences in the contact condition between the H-shaped steel and concrete materials yield differences in stiffness thereafter. The stiffness of model S approximates most closely the experimental result. Therefore, tiebreak contact can yield a decrease in stiffness and a maximum load-carrying capacity because model S can express the occurrence of gaps between the H-shaped steel and the concrete materials.

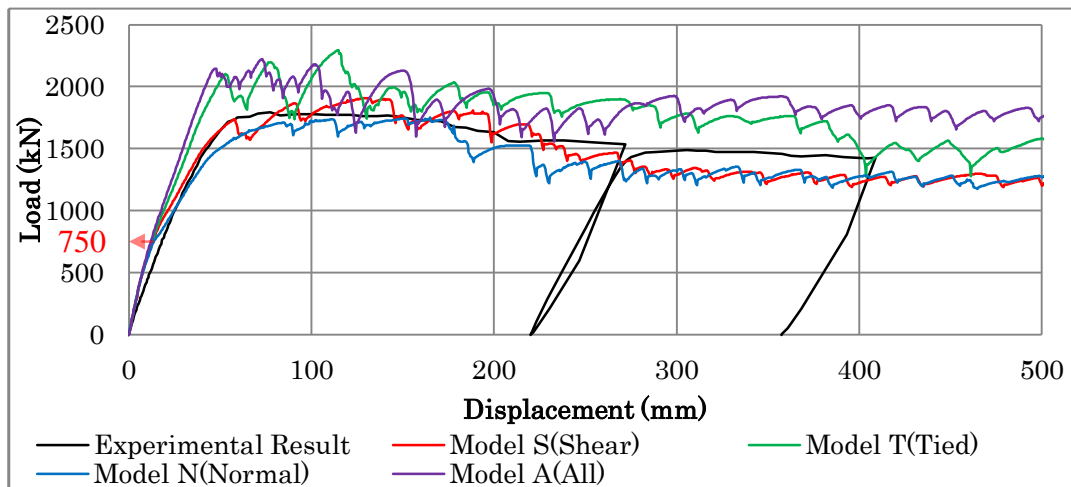


Figure 5. The load-displacement relation of the testing girder.

### 5.2 Testing Slab

Figure 6 shows the load–displacement relationship of the testing slab. The load–displacement relationship is more stable than that of testing girder. It is considered the slippage of the interface between the outer steel plates and supporting points hardly occur because the loading force is small. Model S shows good agreement with the experimental result in terms of the maximum load-carrying capacity. However, model S-without is similar to the experimental result with regards the softening behavior. Connection steels can keep inhibiting the occurrence of gaps between concrete materials until a maximum load is reached. Also, they can increase the maximum load-carrying capacity by 11% compared with the model S-without. Results in the elastic-region indicate that the stiffness of the numerical results is higher than that of the experimental results. Moreover, differences in stiffness between the numerical results are

relatively smaller than those between the numerical results of the testing girder. It is assumed that connection steels counteract the effect of contact conditions between concrete materials and H-shaped steel and concrete materials.

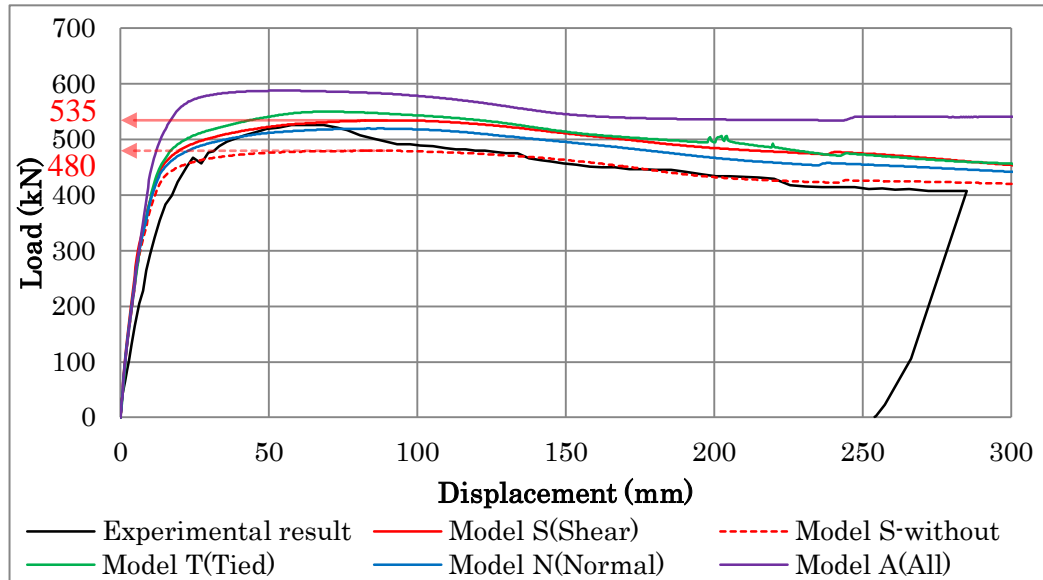


Figure 6. The load-displacement relation of the testing slab.

## 6 CONCLUSION

Tiebreak contact could express a maximum load-carrying capacity. With the testing girder, the stiffness and behavior of the softening could also be obtained. Contact conditions of the interface between the H-shaped steel and concrete materials influenced the numerical results significantly. Therefore, complicated structures such as the SRC rock-shed can be expressed by considering the occurrence of slippage between different materials; tiebreak contact is effective to represent such structures.

From the experimental results, the specimens showed sufficient capacities. With the testing slab, placing connection steels is effective to inhibit the occurrence of gaps between cast-in-place concrete and precast concrete before the maximum load. Such steels can increase the maximum load-carrying capacity by 11% compared with the model S-without.

## REFERENCES

- Bhatti, A.Q., and Kishi, N., Impact Response of RC Rock-shed Girder with Sand Cushion under Falling Load, *Nuclear Engineering and Design*, Elsevier, 240 (10) 2626–2632, October, 2010.
- Committee on Hybrid Structures-Subcommittee on Standard Specification for Hybrid Structures, Series of Fundamental Rule and Design of Standard Specification for Hybrid Structures established in 2014, Japan Society of Civil Engineers, Japan, 2014 (written in Japanese).
- Fukada, S., Kajikawa, Y., and Tokuno, M., Structural Behavior of Reinforced Concrete Slab Rigid Frame Bridge with H-shaped Steels, *Eleventh East Asia-Pacific Conference on Structural Engineering and Construction*, EASEC-11, 2008.
- Yasui, K., Shear Bond Strength of Self-Compacting Mortar (written in Japanese), March, 2010 Retrieved from <http://www.kochi-tech.ac.jp/library/ron/2009/g19/M/1125134.pdf> on December 1, 2016.